Cell
PRESS

Specific Inhibition of p300-HAT Alters Global Gene Expression and Represses HIV Replication

K. Mantelingu,[1,7] B.A. Ashok Reddy,[1,7] V. Swaminathan,[1] A. Hari Kishore,[1] Nagadenahalli B. Siddappa,[2] G.V. Pavan Kumar,[3] G. Nagashankar,[1] Nagashayana Natesh,[4] Siddhartha Roy,[5] Parag P. Sadhale,[6] Udaykumar Ranga,[2] Chandrabhas Narayana,[3] and Tapas K. Kundu[1,*]

[1] Transcription and Disease Laboratory, Molecular Biology and Genetics Unit
[2] Molecular Virology Laboratory, Molecular Biology and Genetics Unit
[3] Light Scattering Laboratory, Chemistry and Physics of Materials Unit
Jawaharlal Nehru Centre for Advanced Scientific Research, Jakkur P.O. Bangalore, India
[4] Central Government Health Scheme Dispensary No. 3, Basavanagudi, Bangalore, India
[5] Molecular Biophysics Unit
[6] Department of Microbiology and Cell Biology
Indian Institute of Science, Bangalore, India
[7] These authors contributed equally to this work.
*Correspondence: tapas@jncasr.ac.in

SUMMARY

Reversible acetylation of histone and non-histone proteins plays pivotal role in cellular homeostasis. Dysfunction of histone acetyltransferases (HATs) leads to several diseases including cancer, neurodegenaration, asthma, diabetes, AIDS, and cardiac hypertrophy. We describe the synthesis and characterization of a set of p300-HAT-specific small-molecule inhibitors from a natural nonspecific HAT inhibitor, garcinol, which is highly toxic to cells. We show that the specific inhibitor selectively represses the p300-mediated acetylation of p53 in vivo. Furthermore, inhibition of p300-HAT down regulates several genes but significantly a few important genes are also upregulated. Remarkably, these inhibitors were found to be nontoxic to T cells, inhibit histone acetylation of HIV infected cells, and consequently inhibit the multiplication of HIV.

INTRODUCTION

Eukaryotic genome is organized in a highly complex nucleoprotein structure, chromatin. Physiologically chromatin is not just DNA and histone complex but rather is a dynamic organization of DNA associated with histone and histone-interacting nonhistone proteins [1]. The hallmark of chromatin is its dynamic nature, which is essential for the regulation of nuclear processes that require access to the genetic information. Several strategies exist to alter the dynamic properties of chromatin including posttranslational modifications of histone and nonhistone chromatin components. Among the different posttranslational modifications, reversible acetylation of histones and different nonhistone nuclear proteins play a significant role

to maintain the nuclear functions. Two groups of enzymes, namely, histone acetyltransferases (HATs) and deacetylases (HDACs), balance the acetylation level as required for cellular function [2]. Based on the protein homology, substrate specificity, and functional consequences, nuclear HATs can be broadly classified under different heads: (1) p300/CBP family; (2) MYST family that consists of Sas2, Sas3, Esa1, MOF, Tip60, MOZ, MORF, HBO1; (3) the GNAT superfamily that includes Hat1, Gcn5, PCAF, Elp3, Hpa2; (4) Nuclear receptor coactivators like SRC-1, ACTR, TIF2; (5) TAFII250 family; and (6) TFIIIC family [3].

p300 and its close homolog CBP are probably the most widely studied histone acetyltransferases. It has been implicated in a number of diverse biological functions such as proliferation, cell-cycle regulation, apoptosis, differentiation, and DNA damage response [4, 5]. It is a potent transcriptional coactivator, which interacts with constantly expanding array of transcription factors [6, 7]. Both p300 and CBP have been found to possess intrinsic HAT activity [8, 9]. Unlike, most of the other HATs that have limited substrate specificity for histone and nonhistone proteins, p300 and CBP are capable of acetylating all the four core histones and also a wide variety of nonhistone proteins with functional consequences in several cases [10]. p300 is a multifunctional protein and all the functions are not HAT activity dependent. However, several important cellular functions are regulated by p300-mediated protein (both histone and nonhistone) acetylation including DNA repair, cell cycle, differentiation, and establishment of retroviral pathogenesis [11, 12].

Lysine-specific acetylation of histone H3 and H4 by p300 in conjunction with chromatin remodeling and other covalent modifications establishes the active state of a chromatin in a gene-specific manner [13]. p300-mediated acetylation of nucleosome-1 (nuc-1) in the integrated HIV genome is essential for the viral gene expression. Furthermore, acetylation of Tat and HIV-1 integrase were also found to be indispensable for the establishment of

viral pathogenesis [14, 15]. Apart from Tat or Integrase, there are several nonhistone nuclear proteins that get acetylated by p300, and as result of which, the functional properties of these proteins are altered. The tumor suppressor p53 gets acetylated by p300 at K373/K382 and by PCAF at K320 residues. The lysine acetylation at these sites of p53 is linked to its ability to regulate cell cycle and apoptosis [16]. In response to DNA damage, N terminus of p53 first becomes phosphorylated at serine 33 and 37, and as a consequence, phosphorylated p53 activates p300 and PCAF to induce p53 acetylation at K373/382 and K320, respectively [17]. However, though acetylation of histone and nonhistone proteins is predominantly associated with transcriptional activation, it is not exclusive. It is evident that p300 acetyltransferase activity is essential for transcriptional repression by promyelocytic leukemia zinc finger (PLZF) protein and HDAC1 [18, 19] (see Discussion).

Because of its involvement in these important cellular events, dysfunction of p300 may be the underlying causes of several diseases, including a few types of cancers, cardiac hypertrophy, asthma, and diabetes [4, 20, 21]. HAT activity of p300 therefore is being considered as a target for the new generation therapeutics. Unlike histone deacetylase inhibitors, the number of HAT modulators (activator and inhibitors) discovered so far is scanty. Among the synthetic HAT modulators, the first group to be described was the Peptide Co-A conjugates, of these Lys Co-A was specific for p300, and H3 Co-A20 was specific for PCAF [22]. Furthermore, γ-butyrolactones were found as first-known small-molecule inhibitors of human Gcn5 HAT activity [23]. Recently, isothiazolones-based modulators have also been designed that inhibits both p300 and PCAF [24]. The search for specific natural small-molecule modulators of HATs succeeded when anacardic acid from cashew nut-shell liquid was found as a potent inhibitor of p300 and PCAF. Furthermore, CTPB (N-[4-chloro-3-trifluoromethyl-phenyl]-2-ethoxy-6-pentadecyl-benzamide), an amide derived by using anacardic acid as a synthon, remarkably activates p300 HAT activity. Unfortunately, these compounds were found to have poor cell-membrane-permeability potential [25]. The lead development in the field was initiated when another natural small-molecule inhibitor of HATs, garcinol, a polyisoprenylated benzophenone derivative from *Garcinia indica* fruit rind was discovered [26]. Garcinol was found to be a nonspecific HAT inhibitor (HATi) but highly permeable to cultured cells and a potent inhibitor of histone acetylation in vivo. The nonspecific nature of garcinol made it highly cytotoxic. Therefore, the potential use of garcinol to target p300 for understanding the physiological role of HATs or to develop a therapeutic molecule is less likely. These limitations of garcinol inspired us to synthesize several derivatives of this potent inhibitor to find out specific and less toxic HAT inhibitors. Among nearly 50 derivatives synthesized from garcinol, three were found to be highly specific for HAT activity of p300. The p300 selectivity was established in vivo by site-specific inhibition of p53 acetylation by one of the inhibitor, LTK-14. The highly

selective nature of LTK-14 prompted us to investigate the role of p300-HAT activity in the regulation of global gene expression. Furthermore, the specific inhibitor was found not only to be nontoxic to T cells but also repressed the HIV replication in these cells. The selective p300 inhibitor thus could be useful as a biological switching molecule for probing the role of p300-HAT in cellular physiology and may also serve as a lead compound to develop new generation therapeutics.

RESULTS

Isogarcinol Derivatives Are Specific Inhibitors of Histone Acetyltransferase p300

The polyisoprenylated benzophenone garcinol isolated from *Garcinia indica* fruit rind was found to be a highly cytotoxic and a nonspecific inhibitor of HATs. In order to find out more potent, specific, and less toxic inhibitors, we synthesized and characterized several derivatives of isogarcinol (IG), a product of intramolecular cyclization of garcinol (Scheme S1 available with this article online). IG was subjected to controlled modification and mono-substitution at "14" position to synthesize 14-isopropoxy IG (LTK-13) and 14-methoxy IG (LTK-14). The disubstitution of IG generated 13, 14 diisopropoxy IG (LTK-13A); 13, 14 dimethoxy IG (LTK-14A); 13, 14 diacetoxy IG (LTK-15); and 13, 14 disulfoxy IG (LTK-19). It was found that the mono substituted IG derivatives LTK-13, -14, and disubstituted LTK-19 could inhibit the p300-HAT activity but not the PCAF-HAT activity (Figure 1A, lanes 5, 6, and 8), although the parent compound IG inhibits HAT activities of both p300 and PCAF nonspecifically (Figure 1A, lane 4). Interestingly, one of the derivatives, LTK-15, almost lost the HAT inhibition activity; it could inhibit the p300-mediated acetylation less than 10% and has no effect on PCAF-HAT activity (Figure 1A, lane 7). Furthermore, the other disubstituted IG derivatives, LTK-13 A and LTK-14 A, also completely lost their activity (data not shown). The IC50 of LTK-13, -14, and -19 to p300-HAT activity were found to be 5–7 μM, which is similar to IG. In order to visualize the inhibition pattern of histone acetylation, HAT assay products were analyzed by fluorography followed by autoradiography. In agreement with filter-binding data, it was found that in the presence of 10 μM of LTK-13, -14, and -19, p300-mediated acetylation of histones H3 and H4 were equally inhibited up to 85%–90% as compared to DMSO solvent control (compare Figure 1B lanes 5, 6, and 8 with lane 3); histone acetylation by PCAF (predominantly at histone H3) was not affected by LTK-13, -14, and -19 (Figure 1C, lanes 5, 6, and 8). As expected, the presence of 10 μM concentration of IG, however, efficiently inhibited histone acetylation by both p300 and PCAF (Figures 1B and 1C, compare lane 3 with 4). However, dose-dependent inhibition of p300-HAT activity was also observed in the presence of LTK-14. Significantly, HAT-activity of PCAF remained unchange even in the presence of 50 μM of LTK14 (Figure S1). In order to ensure the selectivity for p300-HAT activity, we went ahead to check the effect of IG
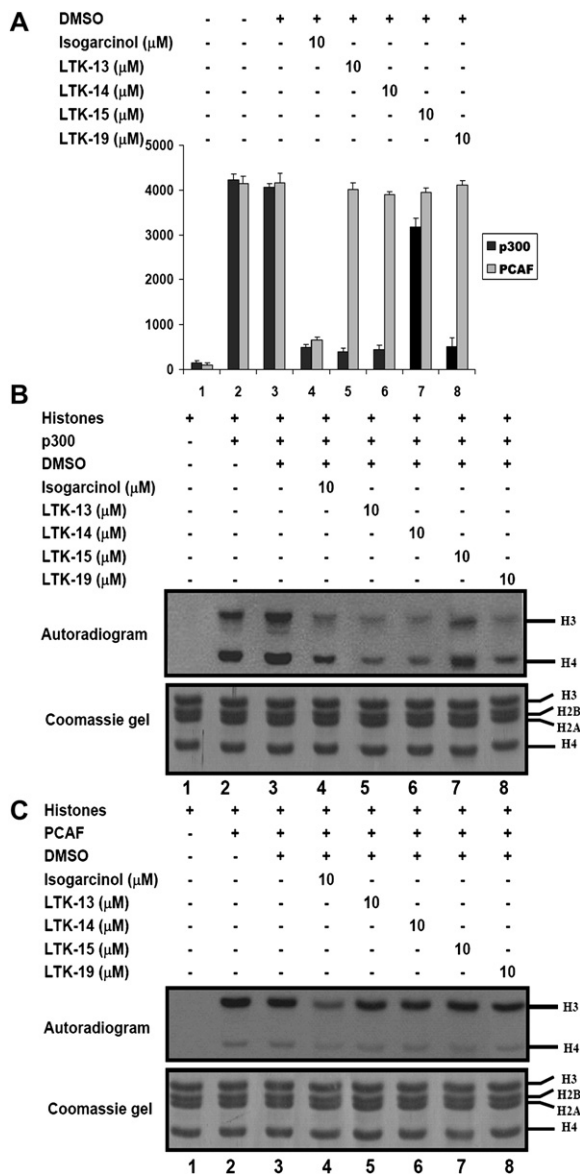
Figure 1. Isogarcinol Derivatives Are Specific Inhibitors of p300-HAT

HAT assays were performed either with p300 or PCAF in the presence and absence of IG or its derivatives by using highly purified HeLa core histones and processed for filter binding (A) or fluorography (B and C). Lane 1, core histones without HAT; lane 2, histones with HAT; lane 3, histones with HAT and in the presence of DMSO; lanes 4–8, histones with HAT and in the presence of IG or its derivatives LTK-13, -14, -15, and -19. Error bars are standard deviation of mean of at least three replicates.

derivatives on the HAT activity of hGcn5, histone deacetylase, HDAC1; arginine methyltransferase, CARM1; and lysine methyltransferase, G9a. Significantly, these chromatin modifying enzyme activities were not affected by the presence of IG and its derivatives LTK-13, -14, and -19 (Figure S2). Taken together, these data suggests that the IG derivatives are specific inhibitors of p300-HAT activity.

p300-Specific Inhibitors Induce Specific Alteration in the Enzyme Conformation as Revealed by Surfaced-Enhanced Raman Spectroscopy

We were further interested to find out whether derivatization of nonspecific compounds alters its functional interaction with the enzyme p300 and also the downstream consequences. Addition of noble metal nanoparticles to biological or chemical molecules produces an enhancement in their Raman intensities and this technique is popularly known as surface-enhanced Raman spectroscopy (SERS). To address this mechanistic aspect, the complex of the compound and the p300 were subjected to SERS investigation. The detailed SERS analysis of p300 molecule has been reported earlier [27]. Figure 2 shows the SERS spectra of p300 and p300 complexes with garcinol, IG, and IG derivatives. The p300 spectrum, as reported earlier, is dominated with the Raman features associated with ring-structured amino acids tryptophan (Trp), tyrosine (Tyr), phenylalanine (Phe), and histidine (His) [27]. p300 is known to contain several units of Trp, Tyr, Phe, and His in it. The spectrum of p300 is also having a prominent Amide I band around 1624 cm^{-1} and 1656 cm^{-1} associated with the α-helix structure. The spectrum of p300 with and without DMSO were found to be quite similar (Figures 2A and 2B), suggesting that there is no contribution from the DMSO to the SERS spectrum of p300. The aromatic ligands, such as garcinol and IG, would form hydrogen bonds and/or have hydrophobic interactions with the protein resulting in the change of the structure of the protein. Since Raman spectrum is closely related to the structure, we expect the changes in Raman spectra upon formation of these complexes. However, there is a small difference in the chemical structures of garcinol and IG molecules, namely, the presence of a hydroxyl group in the garcinol instead of the oxygen bridging in IG as shown in Table 1. Raman spectra of p300 in the presence of these molecules are shown in Figures 2C and 2D. The Raman spectrum of p300 bound with garcinol shows changes mostly to the amide bands of the α-helix, like 1624 cm^{-1} and 1296 cm^{-1}, carboxylic group vibrations of the alphatic amino acids (985 cm^{-1} and 684 cm^{-1}), and certain Tyr modes, like 803 cm^{-1}. On the other hand, IG causes a large-scale change to the p300 spectra. Along with the modes affected in the case of garcinol, the binding of IG also affects all the modes related to Tyr, Trp, Phe, and His. Next, we looked at the derivatives of IG, namely LTK-13, -14, -15, and -19. The Figure 2 shows the SERS spectra of p300 complexes with (Figure 2E) LTK-13, (Figure 2F) LTK-14, (Figure 2G) LTK-19, and (Figure 2H) LTK-15. It is important to note that upon addition of LTK-15, the inactive IG derivative, there is no change to the SERS spectra of p300 (Figure 2H). In the case of LTK-13, the change in the p300 spectra is limited to the amide bands of the α-helix (1656 cm^{-1} and 1517 cm^{-1}) and certain carboxylic groups of the alphatic amino acids (737 cm^{-1} and 617 cm^{-1}). On the other hand, both LTK-14 and -19 causes large-scale changes in the p300 spectra. Like in the case of IG, binding of both LTK-14 and -19 affects not only the amide
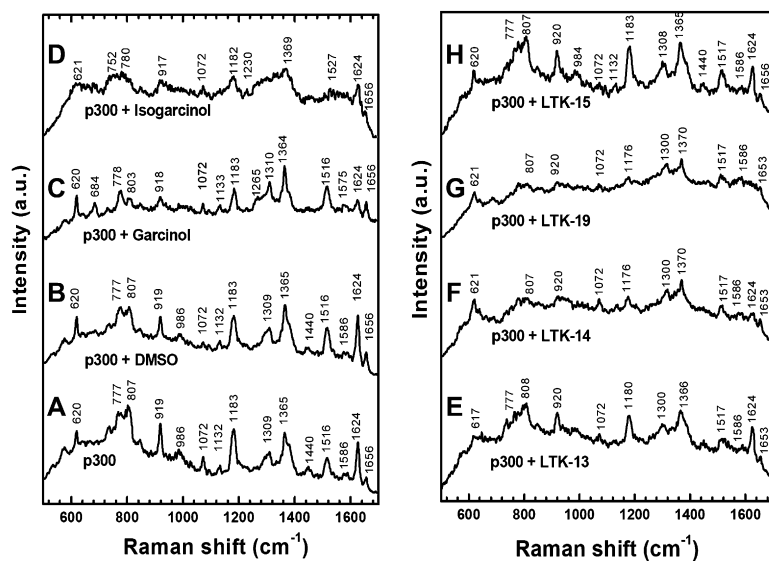
Figure 2. SERS Studies of p300 and Compound Interaction

SERS spectra of (A) p300, (B) p300 + DMSO, (C) p300 + Garcinol, (D) p300 + Isogarcinol, (E) p300 + LTK-13, (F) p300 + LTK-14, (G) p300 + LTK-19, and (H) p300 + LTK-15. Laser excitation, 632.81 nm; laser power at the sample, 8 mW; accumulation time, 180 s.

modes but also all the modes related to Trp, Tyr, Phe, and His. Unlike in the case of IG, in both LTK-14 and -19, the carboxylic side group of the aliphatic amino acid is unaffected, namely, 621 cm^{-1} (compare Figure 2D with Figure 2F and 2G). Taken together, these data suggest that the specific and nonspecific inhibitors of p300 bind to the amide groups of α helix and thereby differentially alter the enzyme structure.

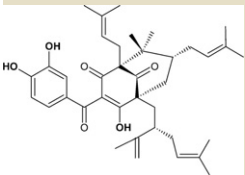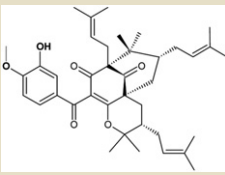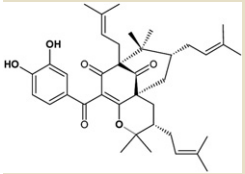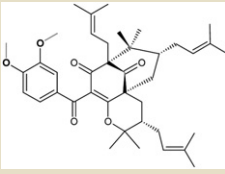## Isogarcinol Derivatives Inhibit the Histone Acetylation In Vivo in HeLa Cells
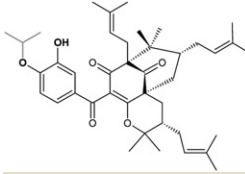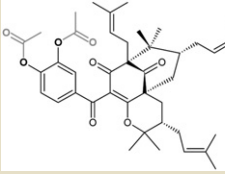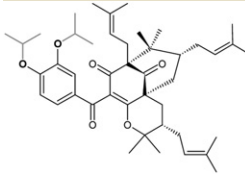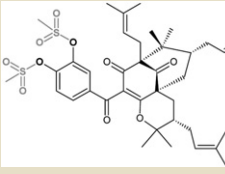
The next question we asked is whether these molecules inhibit the histone acetylation in vivo. In order to investigate the effect of these compounds on the acetylation of histones in vivo, HeLa cells were treated with IG or its derivatives at a concentration of 100 μM for 24 hr. Histones were isolated from control and compound-treated cells and subjected to western blotting analysis with anti-acetyl histone H3 and histone H3 antibodies. Under these experimental conditions, acetylation of histone H3 in untreated as well as DMSO-treated cells could not be detected (Figure 3A, lanes 1 and 2). Therefore, histone acetylation was induced by treating the cells with histone deacetylase inhibitors (NaBu and TSA) (Figure 3A, lanes 3 to 7). In the presence of these inhibitors, cells were treated with IG and its derivatives (100 μM). The results show 70% to 80% inhibition of total acetylation of histones in the case of cells treated with LTK-13, -14, and -19 (Figure 3A, compare lanes 5, 6, and 7 with 3), whereas cells treated with IG show near complete inhibition of total histone acetylation (Figure 3A, compare lane 4 with 3). To visualize the inhibition pattern of histone acetylation in the cells, immunoflurescence studies were carried out by using antiacetyl histone H3 antibodies. Distinct pattern of histone acetylation inhibition was found in the case of cells treated with LTK-14, one of the p300 specific HATi as compared to DMSO (Figure 3B, lane 1, panel I versus II).

Hoechst staining has been shown as control for visualizing nucleus (Figure 3B, lane 2). Merge image shows the distinct inhibition pattern of histone H3 acetylation in vivo upon LTK-14 treatment (Figure 3B, lane 3, panel I versus II). The intensity of the color was quantified and plotted against the length of the image (Figure 3B, lane 4) with a Zeiss LSM.5 Image Examiner. The graphs depict a significant decrease in the histone acetylation (green line) in case of cells treated with LTK-14 as compared to DMSO-treated cells (Figure 3B, lane 4, compare panel I versus II). The blue line represents the nuclei stained with Hoechst. In agreement with western blotting analysis, these data suggest that cells are permeable to these inhibitors and inhibit histone acetylation in vivo.

LTK-14 Inhibits the p300-, but Not PCAF-, Mediated Acetylation of p53

Although in vivo histone acetylation (inhibition) pattern upon treatment with specific inhibitor suggests that the compounds target HAT activity in the cell, the data do not establish the in vivo specificity. To test the specificity of p300-mediated acetylation, we selected p53 as a substrate, which gets acetylated at specific sites by p300 and PCAF very distinctly upon DNA damage. The effect of LTK-14 (Figures 4A and 4B) on acetylation of p53 in vitro was tested by using either p300 or PCAF and bacterially expressed Flag-p53 as substrate. Remarkably, it was observed that LTK-14 inhibited the acetylation of p53 by p300 at 25 μM concentration as compared to DMSO (Figure 4C, compare lane 3 with 4), but the presence of the inhibitor does not affect the p53 acetylation by PCAF (Figure 4C, compare lane 6 with 7). These results suggest that acetylation of p53 by p300 is significantly knocked down in the presence of LTK-14. We further addressed the nature of inhibition in vivo. For this purpose, wild-type p53 expressing A549 human lung carcinoma cells were selected. Cells were treated with the compound

Table 1. Activities and IC50 of HAT Inhibitors

Compound	Specificity	IC50	Cell Toxicity	Compound	Specificity	IC50	Cell Toxicity
Garcinol	Nonspecific	p300, 7 μM; PCAF, 5 μM	Highly toxic	LTK-14	Specific to p300	5–7 μM	Nontoxic
Isogarcinol	Nonspecific	p300, 7 μM; PCAF, 5 μM	Highly toxic	LTK-14A	Inactive	-	Not tested
LTK-13	Specific to p300	5–7 μM	Nontoxic	LTK-15	Inactive	-	Not tested
LTK-13A	Inactive	-	Not tested	LTK-19	Specific to p300	5–7 μM	Nontoxic

for 24 hr following which expression of p53 was enhanced upon treatment with doxorubicin at different time points, 6 and 12 hr. Whole-cell extract was prepared from the cells and subjected to western blotting analysis with antibodies against p53, acetyl p53 (K373), acetyl p53 (K320), and α actin. It was found that at both time points (6 and 12 hr), acetylation of p53 at lysine 373 (by p300) was inhibited by the treatment with LTK-14 (Figure 4D, panel I, lane 1 versus 3 and lane 2 versus 4). Significantly, the specific inhibitor did not affect the acetylation at the lysine 320 (by PCAF) (Figure 4D, panel II, lanes 1 versus 3 and lanes 2 versus 4), whereas presence of IG inhibited the acetylation of p53 at both p300 and PCAF specific sites (Figure S3). Taken together, these results suggest that indeed the inhibitor (LTK-14) obtained by derivatization of IG specifically targets p300 in vivo.

LTK-14 Inhibits p300-HAT Activity-Dependent Chromatin Transcription and Alters Global Gene Expression

In order to find out the effect of p300 specificity of IG derivatives on gene expression, we used the p300-HAT activity-dependent in vitro reconstituted chromatin transcription assay system as described previously [22]. The transcription assay followed the protocol depicted in Figure 5A. Addition of 50 μM concentration of LTK-14 does not show any effect on activator dependent DNA transcription (Figure 5B, lane 6). Even the presence of DMSO, 50 μM concentrations of garcinol and IG did not show any effect on transcription from DNA template (Figure 5B, lanes 3, 4, and 5). The activator-independent transcription from ML 200 promoter was used as a loading control. In this assay system, transcription from the chromatin template is dependent on p300-mediated acetylation of promoter proximal core histones (Figure 5C, lane 3 versus 4) [6]. Addition of DMSO marginally enhances the transcription from the chromatin template (Figure 5C, lane 4 versus 5). However, the presence of 50 μM concentration of LTK-14 shows 70% to 80% inhibition of transcription from chromatin template (Figure 5C, compare lane 5 with 8). Presence of similar concentrations of nonspecific HAT inhibitors, garcinol and IG, show near complete inhibition of transcription (Figure 5C, compare lane 5 with 6 and 7). This could be because garcinol and IG
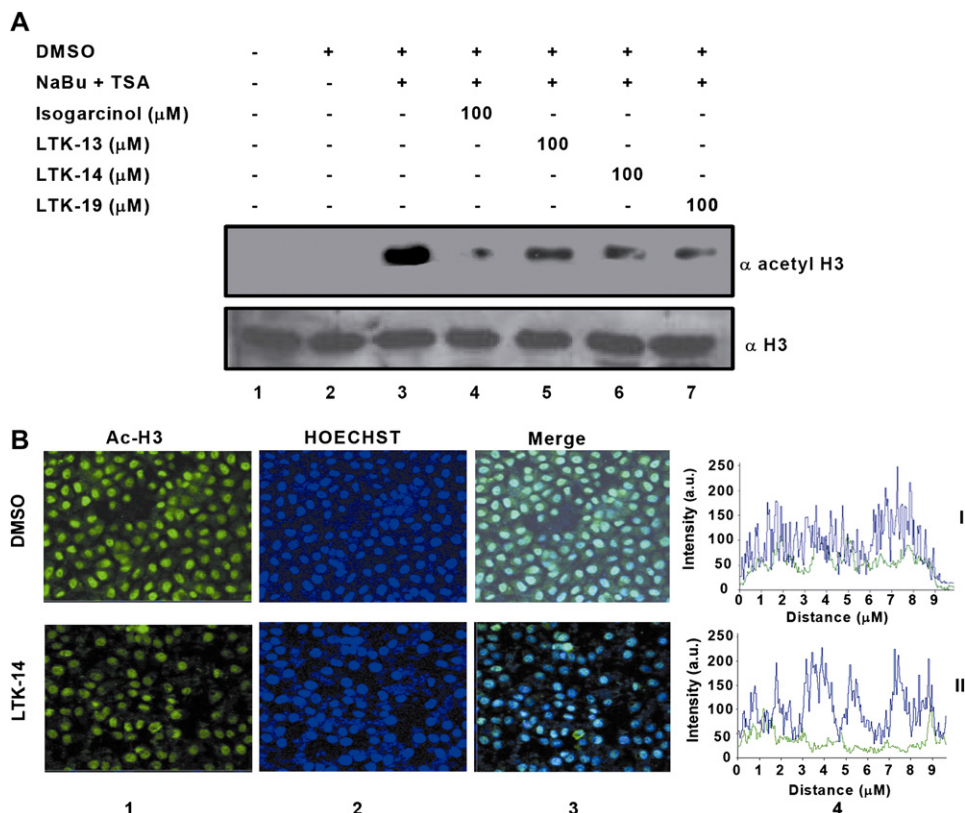
Figure 3. Isogarcinol Derivatives Inhibit Histone Acetylation In Vivo in HeLa Cells

(A) HeLa cells were treated as indicated for 24 hr; lane 1, histones extracted from untreated cells; lane 2, DMSO treated cells; lane 3, NaBu- (1 mM) and TSA- (2 μM) treated cells; lane 4, NaBu- (1 mM), TSA- (2 μM) and IG-treated cells; lanes 5, 6, and 7, cells treated with NaBu (1 mM) and TSA (2 μM) and LTK-13, -14, or -19 respectively. The acid extracted histones were resolved over 12% SDS-PAGE and subjected to western analysis with antibodies against acetylated histone H3.

(B) Inhibition of histone acetylation in HeLa cells by LTK-14 was visualized by immunofluorescence with antiacetyl histone H3 antibodies. Panel I represents cells treated with DMSO, and panel II represents cells treated with LTK-14 (100 μM). Lane 1, stained with acetyl histone H3 antibody; lane 2, cells stained with Hoechst; lane 3, merge image of lanes 1 and 2; lane 4, quantitative representation of lanes 1 and 2.

inhibit all the HATs present in the nuclear extract in addition to p300, but LTK-14 inhibits only p300 but not the other HATs present in the nuclear extract. However, inhibition of p300-HAT activity-dependent chromatin transcription by LTK-14 encouraged us to investigate the effect of p300 inhibition on the global gene expression. For this purpose, HeLa cells were treated with 100 μM LTK-14 for 24 hr and subjected to microarray analysis. Genome-wide analysis of gene expression indicated that a large number of genes were downregulated (118 genes). Remarkably, a few genes were also upregulated upon the inhibition of p300-HAT activity (see Discussion). We have clustered genes according to the level of expression (Figure 5D). An extensive table with all the differentially expressed genes tabulated is available (Table S1). The results were further validated by real-time PCR analysis (Figure 5E).

LTK-14 Inhibits HIV Multiplication in T Cells

Garcinol and IG were found to be highly toxic, presumably because of their nonspecific nature. Importantly, we found that the specific derivatives are significantly less toxic to

HeLa cells as compared to the parent compounds (Figure S4). Furthermore, these derivatives were also found to be nontoxic to T cells up to 50 μM concentration (Figure 6A). These results prompted us to test the p300 specific, nontoxic derivatives on HIV multiplication in T cells. We tested the effect of specific derivative, LTK-14 on virus syncytia formation upon infection on SupT1 cells. SupT1 cells are highly permeable for HIV-1, and these cells make numerous and large syncytia when infected with the virus. Taking advantage of this property, we cocultured SupT1 cells in the presence of H9/HTLV-IIIb NIH 1983 cells that produce a T cell tropic virus. A dose-dependent reduction in the number of syncytia as well as the production of HIV core protein p24 was evident with increasing concentration of LTK-14 (Figures 6B–6D). The difference between treated cells with control was statistically significant at all the time points as evaluated by Student's paired t test (p < 0.005). However, LTK-14 could inhibit the acetylation of histones in T cells significantly (Figure 6E, compare lanes 1, 2, and 3 with 4–12). These results show that the p300-specific HAT inhibitor
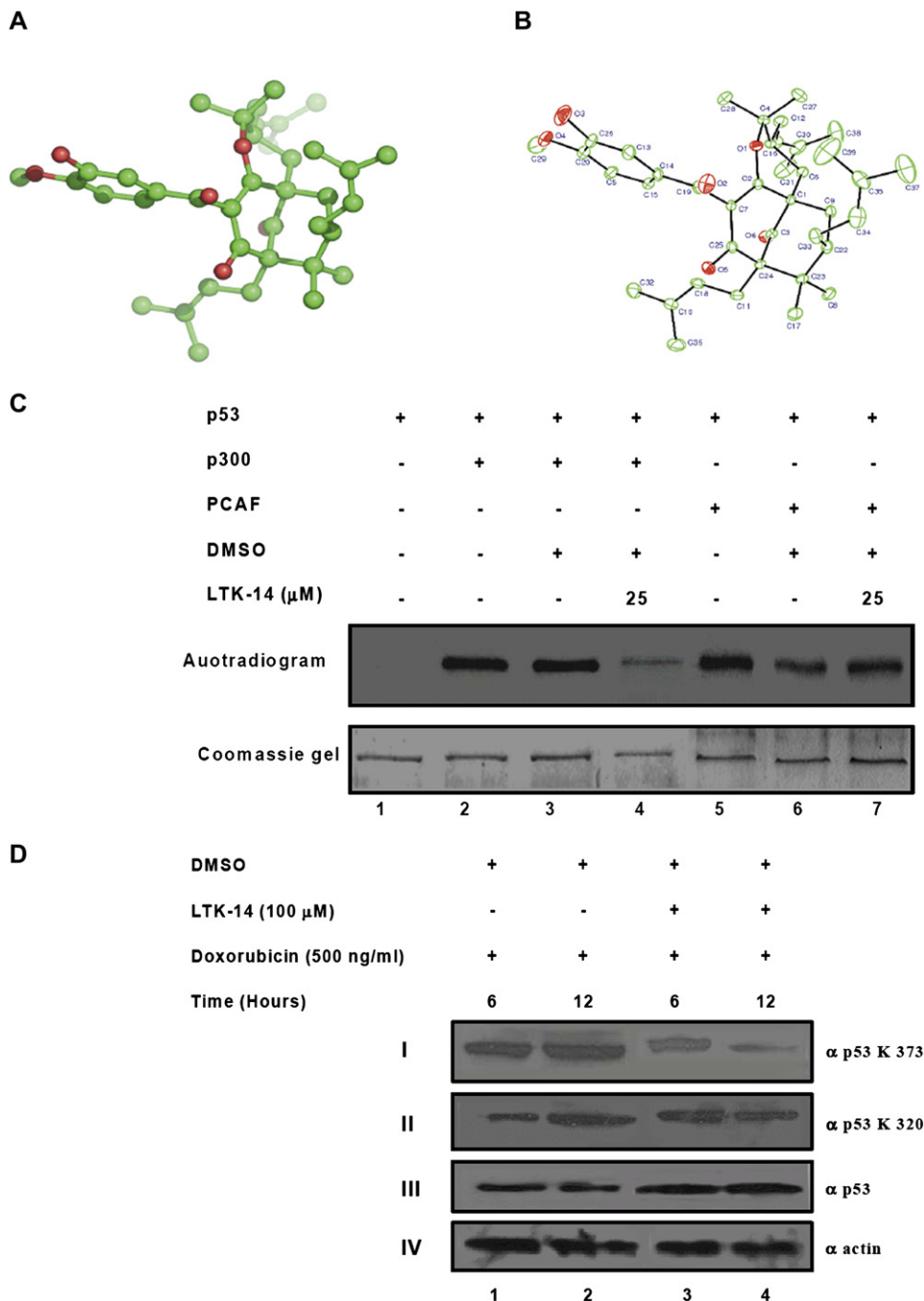
Figure 4. LTK-14 Specifically Inhibits p300-Mediated Acetylation of p53

X-ray crystal structure of LTK-14. (A) Ball-and-stick representation generated by Pymol (hydrogen atoms are not shown for clarity). (B) ORTEP diagrams showing the displacement Ellipsoids are at the 10% probability level. Color coding of the atoms; green represents carbon atoms, and red represents oxygen. (C) In vitro acetyltransferase assays were performed either with p300 or PCAF in the presence or absence of LTK-14 by using Flag-tagged p53 as a substrate. Lane 1, p53 without enzymes; lane 2, p53 in the presence of p300: lane 3, p53 with p300 in the presence of DMSO; lane 4, p53 with p300 in the presence of LTK-14; lane 5, p53 with PCAF; lane 6, p53 with PCAF in the presence of DMSO; lane 7, p53 with PCAF in the presence of LTK-14. Bottom panel represents Coomassie-stained proteins as loading control. (D) A549 cells were treated with either DMSO or LTK-14 for 24 hr. Cells were then incubated with doxorubicin. Lanes 1 and 2, cells treated with DMSO, and lanes 3 and 4, cells with LTK-14, followed by doxorubicin for indicated time points. The cell lysates from the above treatments were probed with a anti acetyl p53 K373 (panel I) and anti acetyl p53 K320 (panel II), anti p53 DO-1 (panel III) and anti actin (panel IV).
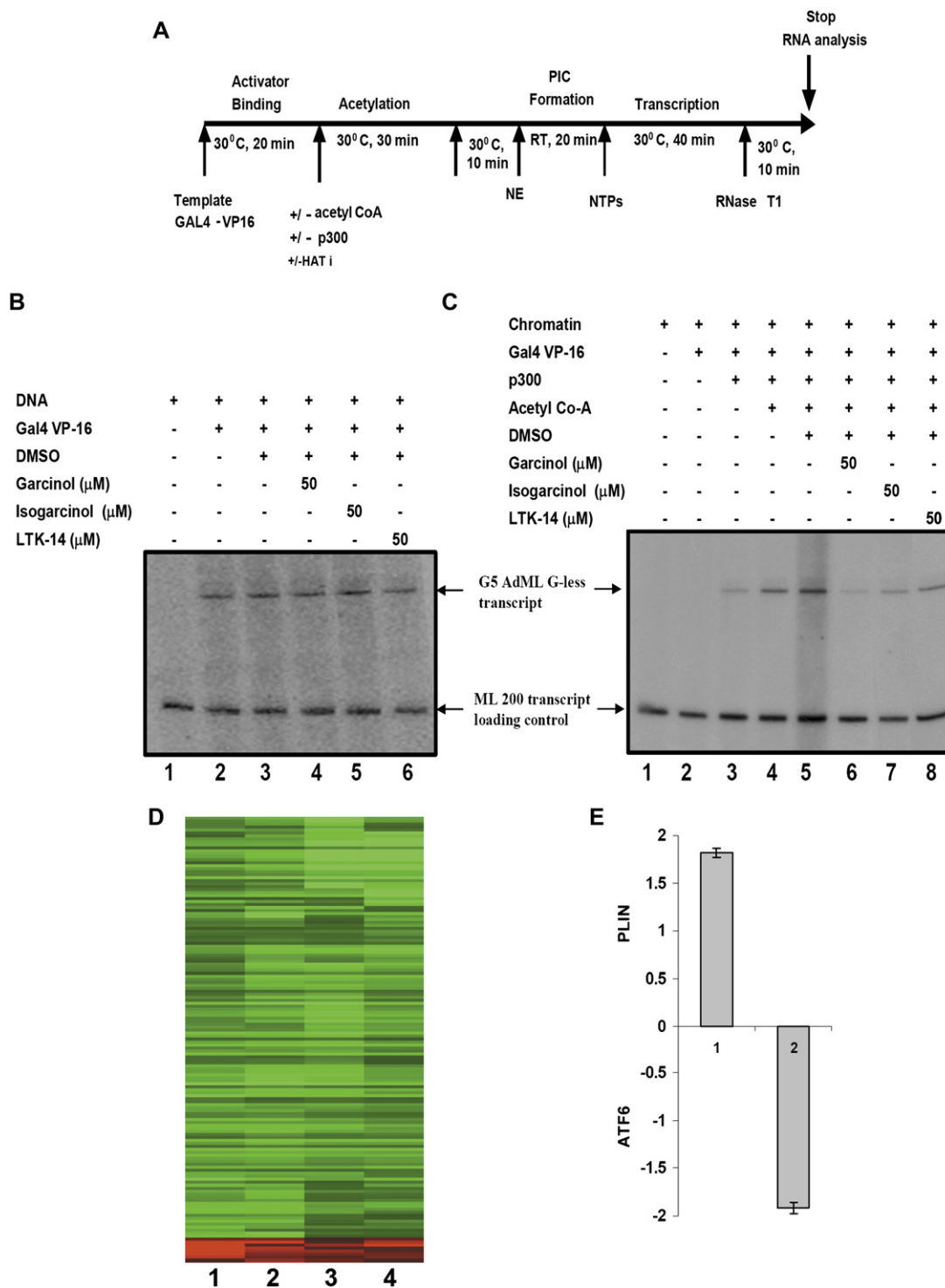
Figure 5. LTK-14 Inhibits the p300-HAT Activity-Dependent Chromatin Transcription In Vitro and Alters Global Gene Expression in HeLa Cells

Schematic representation of the in vitro transcription protocol (A), in vitro transcription from naked DNA (B), and chromatin template (C). Thirty nanograms of DNA and freshly assembled chromatin template (equal amount of 30 ng of DNA) were subjected to protocol (A) with or without HATi. (D) Microarray analysis of gene expression upon treatment of HeLa cells with p300-specific inhibitor LTK-14. Hierarchical clustering of gene expression profile data obtained by cDNA microarray analysis upon inhibition of p300-HAT. Lanes 1 and 2 represents forward reaction, and 3 and 4 represent dye swap. (E) Validation of differentially altered genes by using real-time PCR: PLIN represents upregulated gene, and ATF6 downregulated gene. Error bars are standard deviation of mean of at least three replicates.
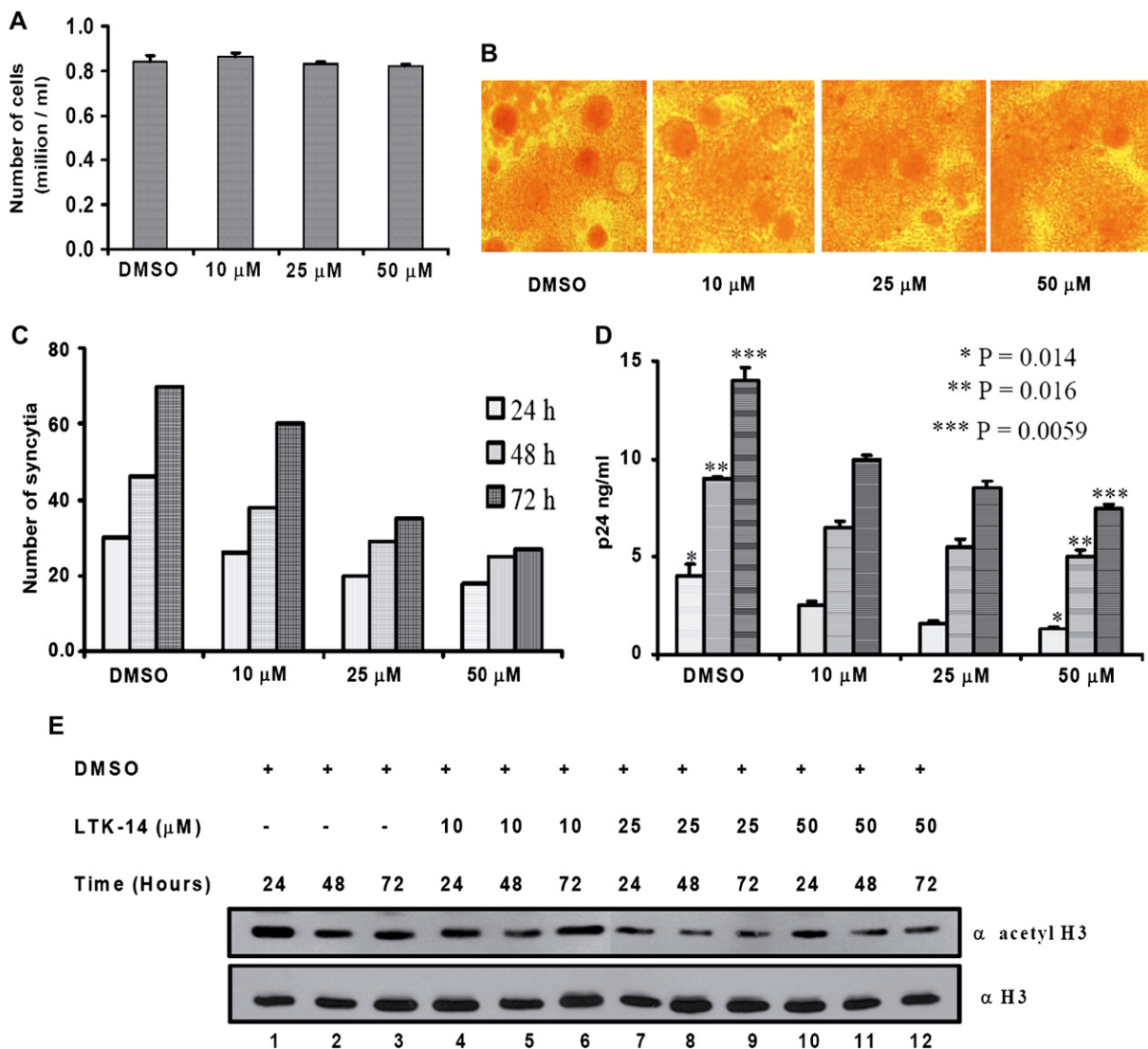
Figure 6. Nontoxic p300-Specific Inhibitor LTK-14 Represses HIV Multiplication through the Inhibition of Histone Acetylation in T Cells

(A) Trypan blue cell viability assay was carried out to determine the toxicity of LTK-14 to T cells. Lane 1, DMSO treated cells; lanes 2, 3, and 4, treated with LTK-14, at 10, 25, and 50 μM concentrations, respectively. Three individual experiments were carried out, and percent cell death was calculated and plotted against each treatment.

(B) LTK-14 was added to the wells to the final concentration as shown, and the cultures were incubated at 37°C. Formation of syncytia is visible under light microscope within 12 hr.

(C) The total number of syncytia in ten representative wells was counted and presented. The data are representative of three independent experiments.

(D) The viral structural protein, p24, secreted into the culture medium was estimated by using an antigen-capture assay. The difference between cells treated with control and 50 μM concentration was found to be statistically significant by Student's paired t test. Error bars are standard deviation of mean of at least three replicates.

(E) Inhibition of histone acetylation in the infected T cells was visualized by western blotting with antiacetylated histone H3 antibodies. Cells were treated with 10, 25, and 50 μM concentration of compound for 24, 48, and 72 hr as indicated. Histones isolated from the above treatments were subjected to western blotting.

LTK-14 inhibits the multiplication of HIV at least partially, through the inhibition of acetylation of histones.

DISCUSSION

Though the existence of HATs has been known for nearly 40 years, the recombinant HATs, initially Gcn5 and then p300/CBP were discovered only a decade ago. Availability of the recombinant enzymes enabled the synthesis of the HAT-specific modulators, especially inhibitors [22]. However, it was challenging to find out the natural molecules, which have the HAT-modulating activity. The first known cell-permeable small-molecule HAT inhibitor is garcinol, an isoprenylated benzophenone

derivative isolated from *Garcinia indica* fruit rind. Garcinol was found to be highly potent nonspecific HAT inhibitor, which inhibits histone acetylation in vivo and induces apoptosis [26]. These results are in agreement with the notion that natural products often demonstrate nonselective and broad-range activity against several classes of enzymes with high affinity; therefore, they are likely to be cytotoxic to mammalian cells. This phenomenon provides an opportunity for chemical biologists to synthesize selective, more potent, and less toxic analogs by small modifications of natural products. In the present report, we synthesized several derivatives of garcinol, to achieve selective inhibition of HAT activity. Upon intramolecular cyclization of garcinol, another nonspecific inhibitor IG was synthesized. Initially, we aimed at synthesizing p300/CBP-specific inhibitor. Nonavailability of the 3D structure of the enzyme was limiting factor for synthesis of structure-based ligands. However, monosubstitution or disubstitution by electron donor or electron withdrawing functional groups at 14 and/or 13 oxygen atoms was considered as a potential strategy for synthesizing different IG derivatives. Significantly, out of several derivatives synthesized, three (LTK-13, -14, and -19) showed exclusive specificity for p300-HAT activity. With the exception of the sulphonyl group disubstitution, all the other disubstitutions would fail to confer the specificity to the derivatives. For example, disubstitution by acetyl moiety resulted in a loss of activity (LTK-15). Molecular interactions of p300 with different derivatives was investigated by using surface-enhanced Raman spectroscopy studies, which clearly showed that the mode of interaction and consequent alteration of enzyme structure of specific versus nonspecific inhibitors differ significantly (Figure 2). Furthermore, the inactive inhibitor seems to have lost the ability to interact with the enzymes (Figure 2H). LTK14 could not affect the autoacetylation of p300, within the concentration range of the HAT inhibition (data not shown). The kinetics data suggests that the specific inhibitor (LTK-14) mediated inhibition pattern is significantly different from the nonspecific parent compound. It is a mixed type for both histones as well as acetyl Co-A, whereas garcinol was found to be a competitive for histones and mixed type for acetyl Co-A (Figure S5). Presumably, the inhibitor binds to specific pocket of the enzyme other than the active site. Therefore, specific alteration of enzyme structure by the derivatives might have lead to the selective inhibition of p300-HAT activity.

The p300-mediated acetylation regulates the tumor suppressor functions not only through the acetylation of histones but also through the acetylation of p53. Role of p53 acetylation in cellular gate-keeping functions is controversial [16, 28]; however, the significant implication of it is beyond doubt. p53 gets reversibly acetylated at C terminus by p300 and PCAF in a site-specific manner. Functional significance of each of these site-specific acetylations is yet to be established in the context of p53-mediated cell-cycle arrest or apoptosis. We found that LTK-14 remarkably inhibits only p300-mediated p53 acetylation in vitro as well as in vivo (Figures 4C and 4D).

These data establish that LTK-14 is indeed a p300-specific inhibitor.

Through its intrinsic HAT activity, p300 play significant role in the transcriptional activation from the chromatin, which is the major molecular basis for its function [6]. Having recruited by the transcriptional activator, p300 acetylates the promoter proximal histones and thereby facilitates transcription initiation. We found that LTK-14 inhibits the acetylation-dependent (by p300) chromatin transcription in vitro (Figure 5C). Microarray analysis of the p300 selective inhibitor (LTK-14)-treated cells resulted in a large number (118) of downregulated genes. Significantly, a few (six) important genes were also upregulated (Figure 5D). Among the downregulated genes, many are involved in different cellular functions such as cell cycle (*HSP90B1*) [29], differentiation (*CAST* [30]), proliferation (*BECN1* [31]), and apoptosis (*ATF6* [32]). These results may be useful to identify the molecular target of p300 for cell growth, differentiation, and death. A few downregulated genes such as *MAPK8IP1* (mitogen-activated protein kinase 8-interacting protein 1) and *HSP90B1* are signal sensors involved in key cellular signaling processes [33, 34]. Interestingly, couple of oncogenes such as, *MYC* [35], *V-Yes-1* [36], and *RAS25* (RAS oncogene homolog) [37] were downregulated. Furthermore, many genes involved in diseases like diabetes (*MAPK8IP1* [38]), asthma (*HSPG2* [Perlecan] [39]), heart and cardiomyopathy (*MYO6* [40]), and cancer (*DIABLO* [41]) were downregulated. These results further establish that p300 is indeed a molecular target for many diseases. Among the upregulated genes, few are involved in cell growth and differentiation (*GLDN* [42]), metabolism (*PLIN* [43]), and cell signaling (*PLIN* [43]). Interestingly, the upregulated gene *PLIN* is involved in diabetes and obesity-related disorders [44]. Several genes with unknown function were altered upon p300 inhibition; analysis of these genes would be helpful to assign new roles for p300/CBP (Table S1), and such analysis would be helpful in unraveling the diverse but uncharacterized mechanisms of p300 either in gene activation or repression, ultimately leading to pathogenesis.

Derivatization of IG toward the more selective inhibitory function made these molecules significantly nontoxic to HeLa cells (Figure S4) as revealed by Tryphan blue cell viability assay. Toxicity of these molecules has been considerably reduced also for T cells (Figure 6A) and embryonic stem cells (data not shown). Since p300 mediated acetylation of different HIV proteins (Tat, integrase) as well as nucleosomes on the integrated HIV genome is essential for the multiplication of HIV, we tested the effect of LTK-14 on the viral gene expression. The results demonstrate that viral syncitia formation reduced significantly in the presence of the p300-specific HAT inhibitor (LTK-14) within its nontoxic range of concentration. The inhibition of HIV multiplication was further confirmed by the estimation of viral coat protein p24 production, and the results were found to be statistically significant. Inhibition of HIV multiplication is in agreement with the inhibition of histone acetylation in T cells (Figure 6E). p300-mediated acetylation of HIV-1 integrase is indispensable for the

integration of the provirus into the human genome [15]. Therefore, we presume that inhibition of syncitia formation by the presence of p300-specific inhibitor could also be through the inhibition of acetylation of integrase and its downstream activity that further stops the spread of the infection. The p300-specific inhibitors may act at different stages of HIV life cycle starting from its integration into human genome to gene expression after integration. However, in vivo acetylation status of Tat and HIV-1 integrase could not be tested upon compound treatment because of the limited amount of proteins synthesized in the infected cells.

SIGNIFICANCE

p300 plays a critical role in cell growth, differentiation, and death. Several of these functions require intrinsic HAT activity of p300-HAT. Because of its critical role in diverse cellular functions, dysfunction of p300 may be the underlying cause of many diseases including cancer. p300 also plays a crucial role in the establishment of HIV pathogenesis. However, the molecular basis of p300 contribution toward diverse cellular processes is still unresolved. We have synthesized a few cell-permeable, p300-HAT-specific inhibitors from nonspecific and highly toxic natural HAT inhibitor, garcinol. These specific and nontoxic small molecules would be highly useful to understand the biological roles of HAT function as revealed by our microarray analysis and inhibition of p53 site-specific acetylation. Furthermore, these molecules also hold tremendous therapeutic potential for different diseases including AIDS and cancer.

EXPERIMENTAL PROCEDURES

General Procedure for the Synthesis and Characterization of Derivatives

See the Supplemental Data.

Histone Acetyltransferase Assay

HAT assays were performed as described previously [6]. 1.8 μg of highly purified HeLa core histones were incubated in HAT assay buffer at 30°C for 10 min with or without baculovirus-expressed recombinant p300 or PCAF in the presence and absence of IG derivatives followed by addition of 0.5 μl of 4.7 Ci/mmol [^{3}H] acetyl CoA (NEN-PerkinElmer) and were further incubated for another 10 min in a 30 μl reaction. The reaction mixture was then blotted onto P-81 filter paper (Whatman), and radioactive counts were recorded on a PerkinElmer Wallac 1409 liquid scintillation counter. The radio labeled acetylated histones were visualized by resolving on 15% SDS-polyacrylamide gel and subjected to fluorography followed by autoradiography.

Surface-Enhanced Raman Spectroscopy

Raman spectroscopic studies were carried out on a custom built Raman spectrometer described elsewhere [27]. The laser excitation used was 532 nm from a frequency doubled diode pumped Nd-YAG laser with a maximum power of 8 mW at the sample. The typical accumulation times for each spectrum were 180 s. The silver nanoparticles were prepared by the standard Lee and Meisel method as described earlier [27]. The typical size of the Ag nanoparticles were found to be ~50 nm by transmission electron microscopy. p300

solution (protein concentration ~40 ng/μl) was mixed with Ag nanoparticles solution in the ratio of 1:4 and put on to a cavity glass slide. The mixture was allowed to settle for 5 min before recording the SERS with a water immersion high-magnification objective. To record the p300 spectrum with the inhibitors, a 10 μM solution of IG or its derivative was added to the above mixture.

In Vitro Chromatin Transcription

Chromatin template for in vitro transcription was assembled and characterized as described earlier [6]. Transcription assays were carried out as described earlier [6] with minor modifications. The scheme of transcription is shown in Figure 5A. The experiment is carried out in the presence and absence of 50 μM Garcinol, IG, and LTK-14, and all the steps were followed as described earlier [22].

Analysis of In Vivo Histone Acetylation

HeLa cells (1.5×10^6 cells per 60 mm dish) were seeded overnight, and histones were extracted from 24 hr of compound-treated cells. The quantitated protein samples were run on a 12% SDS-polyacrylamide gel. After electrophoresis, proteins on the gel were electrotransferred onto an Immobilon membrane (polyvinylidene difluoride; Millipore, Corp., Bedford, MA). The membranes were then blocked in 5% nonfat dry milk solution in 1× PBS containing 0.05% Tween 20 and then immunoblotted with anti-acetyl H3, or anti-H3. Detection was performed with goat anti-rabbit secondary antibody (Bangalore Genei), and bands were visualized with the use of the ECL detection system (Pierce).

Immunofluroscence

To visualize the inhibition of histone acetylation in vivo, HeLa cells were cultured as monolayer on the poly L-lysine-coated cover slips in DMEM (Sigma) medium. Immunofluroscence was carried out as described elsewhere [44]. Fixed cells were probed with antiacetylated histone H3 polyclonal antibodies followed by secondary antibodies conjugated with Alexa 488. To stain the chromosomal DNA Hoechst 33528 (Sigma) was used. The images were taken by using Zeiss LSM 510 laser scanning confocal microscope.

p53 Modulation Assays

In vitro p53 acetylation assays were carried out either with p300 or PCAF similarly as HAT assays described above. Flag-tagged p53 was incubated for 10 min in the presence and absence of LTK-14 either with p300 or PCAF. Then 0.5 μl of 4.7 Ci/mmol [^{3}H] acetyl CoA (NEN-PerkinElmer) was added and incubated further for 30 min at 30°C. Then reaction mixtures were subjected to fluorography followed by autoradiography. For in vivo p53 modulation studies, A549 cells were incubated for 24 hr with LTK-14 (100 μM) and DMSO. Cells were then treated with 0.5 μg/ml of doxorubicin for 6 and 12 hr. The cells were harvested and lysed by using TNN buffer (150 mM NaCl, 50 mM Tris [pH 7.4], 1% Nonidet P-40, 0.1% sodium deoxycholate, 1 mM EDTA, 0.5 μg/ml leupeptin, 0.5 μg/ml aprotinin, and 0.5 μg/ml pepstatin), for 3 hr on ice with intermittent mixing. The whole-cell lysates from the above treatments were subjected to western analysis by using mouse monoclonal anti-p53 antibody, DO1 (oncogene), rabbit polyclonal acetylated p53 K373 and K320 (Upstate), and actin (Calbiochem).

Microarray Analysis

The total RNA was isolated from control and treated cells by using the TRIZOL (Invitrogen) method. The Micromax direct labeling kit, MPS502 (PerkinElmer), was used to synthesize the labeled cDNA from 70 μg of total RNA and further process the hybridized cDNA on the array. All the steps were carried out according to manufacturer's instructions (http://las.perkinelmer.com/content/Manuals/MAN_Micro maxDirect50Reactions25Arrays.pdf). The array slides were scanned immediately with a PerkinElmer ScanArray Gx microarray scanner. The ScanArray software (PerkinElmer) was used for grid-wise normalization of array images. Four arrays were used with at least two biological treatments of cells, and dye-swap experiments were included in the final analysis. The data were analyzed by GeneSpring GX and

Biointerpreter softwares from Genotypic Technology, Bangalore. The differential expression was considered if the Log_2 mean of at least -1 for the downregulated genes and $+1$ for the upregulated genes. We considered only the genes that were reproducible from all four replicates.

Real-Time PCR Analysis

cDNA was synthesized from total RNA by using oligo (dT) and SuperScript real-time PCR kit (Invitrogen). The real-time generated cDNA was amplified with gene-specific primers (Sigma-Aldrich), ATF-6 (forward primer 5′-gactctttcacaggctggatg-3′, reverse primer 5′-cttccttcagtggctccgc-3′), PLIN (forward primer- 5′-gagaatgtgctg cagcggg-3′, reverse primer- 5′-gcgggtggagatggtgtc-3′), and iQ SYBR Green Supermix (BioRad). Actin was used as an internal control. PCR analysis was performed with a BioRad iCycler real-time PCR machine.

Syncytium Inhibition Assay and p24 Estimation

The cell lines SupT1 and H9/HTLV-IIIb NIH 1983 were obtained from the NIH AIDS Research and Reference Reagent Program. H9/HTLV-IIIb NIH 1983 cells carrying stably integrated proviruses were cocultured with excess numbers of SupT1 cells at a ratio of 1:200. A total of 1×10^6 cells were seeded in each well of a 24-well plate and cultured in RPMI medium supplemented with 10% fetal calf serum and antibiotics. LTK-14 in DMSO was added to the cells at a range of concentration, and the cultures were incubated at 37°C. All the wells, including the control, received the same amount of DMSO. Formation of syncytia was visible under light microscope within 12 hr. The total number of syncytia in ten representative wells was counted at different time points (24, 48, and 72 hr); data for the 48 hr time point are presented. Identical results were obtained at other time points. Culture supernatant was sampled every 24 hr for p24 analysis. Empigen was added to each sample to a final concentration of 0.1%, and the samples were incubated at 56°C for 30 min to inactivate the virus and to release the p24 antigen. The quantity of p24 in the samples was measured with a commercial kit following manufacturer's instructions (PerkinElmer, Boston, MA). All the assays were performed in triplicate wells, and the experiment was performed two times.

Supplemental Data

Supplemental Data include the Supplemental Experimental Procedures and results of (1) histone deacetylase and methyltransferase assays, (2) expression and purification of proteins, (3) cytotoxic assay, and (4) isolation of garcinol, synthesis of garcinol derivatives, and characterization and X-ray structure determination of LTK-14 and are available at http://www.chembiol.com/cgi/content/full/14/6/645/DC1/.

REFERENCES

1. Batta, K., Das, C., Gadad, S., Shandilya, J., and Kundu, T.K. (2007). Reversible acetylation of nonhistone proteins: role in cellular function and disease. Subcell. Biochem. 41, 193–214.

2. Roth, S.Y., Denu, J.M., and Allis, C.D. (2001). Histone acetyltransferases. Annu. Rev. Biochem. 70, 81–120.

3. Sterner, D.E., and Berger, S.L. (2000). Acetylation of histones and transcription-related factors. Microbiol. Mol. Biol. Rev. 64, 435–459.

4. Iyer, N.G., Ozdag, H., and Caldas, C. (2004). p300/CBP and cancer. Oncogene 23, 4225–4231.

5. Goodman, R.H., and Smolik, S. (2000). CBP/p300 in cell growth, transformation and development. Genes Dev. 14, 1553–1577.

6. Kundu, T.K., Palthan, V.B., Wang, Z., An, W., Cole, P.A., and Roeder, R.G. (2000). Activator-dependent transcription from chromatin in vitro involving targeted histone acetylation by p300. Mol. Cell 6, 551–561.

7. Chan, H.M., Krstic-Demonacos, M., Smith, L., Demonacos, C., and La Thangue, N.B. (2001). Acetylation control of the retinoblastoma tumour-suppressor protein. Nat. Cell Biol. 3, 667–674.

8. Bannister, A.J., and Kouzarides, T. (1996). The CBP co-activator is a histone acetyltransferase. Nature 384, 641–643.

9. Ogryzko, V.V., Schiltz, R.L., Russanova, V., Howard, B.H., and Nakatani, Y. (1996). The transcriptional coactivators p300 and CBP are histone acetyltransferases. Cell 87, 953–959.

10. Das, C., and Kundu, T.K. (2005). Transcriptional regulation by the acetylation of nonhistone proteins in humans—a new target for therapeutics. IUBMB Life 57, 137–149.

11. Giordano, A., and Avantaggiati, M.L. (1999). p300 and CBP: partners for life and death. J. Cell. Physiol. 181, 218–230.

12. Quivy, V., and Van Lint, C. (2002). Diversity of acetylation targets and roles in transcriptional regulation: the human immunodeficiency virus type 1 promoter as a model system. Biochem. Pharmacol. 64, 925–934.

13. Barrero, M.J., and Malik, S. (2006). Two functional modes of a nuclear receptor-recruited arginine methyltransferase in transcriptional activation. Mol. Cell 24, 233–243.

14. Varier, R.A., and Kundu, T.K. (2006). Chromatin modifications (acetylation/deacetylation/methylation) as new targets for HIV therapy. Curr. Pharm. Des. 12, 1975–1993.

15. Cereseto, A., Manganaro, L., Gutierrez, M.I., Terreni, M., Fittipaldi, A., Lusic, M., Marcello, A., and Giacca, M. (2005). Acetylation of HIV-1 integrase by p300 regulates viral integration. EMBO J. 24, 3070–3081.

16. Knights, C.D., Catania, J., Di Giovanni, S., Muratoglu, S., Perez, R., Swartzbeck, A., Quong, A.A., Zhang, X., Beerman, T., Pestell, R.G., et al. (2006). Distinct p53 acetylation cassettes differentially influence gene-expression patterns and cell fate. J. Cell Biol. 173, 533–544.

17. Sakaguchi, K., Herrera, J.E., Saito, S., Miki, T., Bustin, M., Vassilev, A., Anderson, C.W., and Appella, E. (1998). DNA damage activates p53 through a phosphorylation-acetylation cascade. Genes Dev. 12, 2831–2841.

18. Guidez, F., Howell, L., Isalan, M., Cebrat, M., Alani, R.M., Ivins, S., Hormaeche, I., McConnell, M.J., Pierce, S., Cole, P.A., et al. (2005). Histone acetyltransferase activity of p300 is required for transcriptional repression by the promyelocytic leukemia zinc finger protein. Mol. Cell. Biol. 25, 5552–5566.

19. Qiu, Y., Zhao, Y., Becker, M., John, S., Parekh, B.S., Huang, S., Hendarwanto, A., Martinez, E.D., Chen, Y., Lu, H., et al. (2006). HDAC1 acetylation is linked to progressive modulation of steroid receptor-induced gene transcription. Mol. Cell 22, 669–679.

20. McKinsey, T.A., and Olson, E.N. (2004). Cardiac histone acetylation—therapeutic opportunities abound. Trends Genet. *20*, 206–213.

21. Barnes, P.J., Adcock, I.M., and Ito, K. (2005). Histone acetylation and deacetylation: importance in inflammatory lung diseases. Eur. Respir. J. *25*, 552–563.

22. Lau, O.D., Kundu, T.K., Soccio, R.E., Ait-Si-Ali, S., Khalil, E.M., Vassilev, A., Wolffe, A.P., Nakatani, Y., Roeder, R.G., and Cole, P.A. (2000). HATs off: selective synthetic inhibitors of the histone acetyltransferases p300 and PCAF. Mol. Cell *5*, 589–595.

23. Biel, M., Kretsovali, A., Karatzali, E., Papamathekis, J., and Giannis, A. (2004). Design, synthesis and biological evaluation of a small-molecule inhibitor of the histone acetyltransferase Gcn5. Angew. Chem. Int. Ed. Engl. *43*, 3974–3976.

24. Stimson, L., Rowlands, M.G., Newbatt, Y.M., Smith, N.F., Raynaud, F.I., Rogers, P., Bavetsias, V., Gorsuch, S., Jarman, M., Bannister, A., et al. (2005). Isothiazolones as inhibitors of PCAF and p300 histone acetyltransferase activity. Mol. Cancer Ther. *4*, 1521–1532.

25. Balasubramanyam, K., Swaminathan, V., Ranganathan, A., and Kundu, T.K. (2003). Small molecule modulators of histone acetyltransferase p300. J. Biol. Chem. *278*, 19134–19140.

26. Balasubramanyam, K., Altaf, M., Varier, R.A., Swaminathan, V., Ravindran, A., Sadhale, P.P., and Kundu, T.K. (2004). Polyisoprenylated benzophenone, garcinol, a natural histone acetyltransferase inhibitor, represses chromatin transcription and alters global gene expression. J. Biol. Chem. *279*, 33716–33726.

27. Pavan Kumar, G.V., Ashok Reddy, B.A., Arif, M., Kundu, T.K., and Narayana, C. (2006). Surface-enhanced Raman scattering studies of human transcriptional coactivator p300. J. Phys. Chem. B *110*, 16787–16792.

28. Zhao, Y., Lu, S., Wu, L., Chai, G., Wang, H., Chen, Y., Sun, J., Yu, Y., Zhou, W., Zheng, Q., et al. (2006). Acetylation of p53 at lysine 373/382 by the histone deacetylase inhibitor depsipeptide induces expression of p21(Waf1/Cip1). Mol. Cell. Biol. *26*, 2782–2790.

29. Liu, G., and Lozano, G. (2005). p21 stability: linking chaperones to a cell cycle checkpoint. Cancer Cell *7*, 113–114.

30. Xu, Y., and Mellgren, R.L. (2002). Calpain inhibition decreases the growth rate of mammalian cell colonies. J. Biol. Chem. *277*, 21474–21479.

31. Yu, L., Lenardo, M.J., and Baehrecke, E.H. (2004). Autophagy and caspases: a new cell death program. Cell Cycle *3*, 1124–1126.

32. Nakanishi, K., Sudo, T., and Morishima, N. (2005). Endoplasmic reticulum stress signaling transmitted by ATF6 mediates apoptosis during muscle development. J. Cell Biol. *169*, 555–560.

33. Lee, C.W., Lin, W.N., Lin, C.C., Luo, S.F., Wang, J.S., Pouyssegur, J., and Yang, C.M. (2006). Transcriptional regulation of VCAM-1 expression by tumor necrosis factor-alpha in human tracheal smooth muscle cells: involvement of MAPKs, NF-kappaB, p300 and histone acetylation. J. Cell. Physiol. *207*, 174–186.

34. Simonsson, M., Kanduri, M., Gronroos, E., Heldin, C.H., and Ericsson, J. (2006). The DNA binding activities of Smad2 and Smad3 are regulated by coactivator-mediated acetylation. J. Biol. Chem. *281*, 39870–39880.

35. Al-Kuraya, K., Novotny, H., Bavi, P.P., Siraj, A.K., Uddin, S., Ezzat, A., Al Sanea, N., Al-Dayel, F., Al-Mana, H., Sheikh, S.S., et al. (2006). HER2, TOP2A, CCND1, EGFR and C-MYC oncogene amplification in colorectal cancer. J. Clin. Pathol., in press. Published online August 1, 2006. 10.1136/jcp.2006.038281.

36. Sudol, M., Kuo, C.F., Shigemitsu, L., and Alvarez-Buylla, A. (1989). Expression of the yes proto-oncogene in cerebellar Purkinje cells. Mol. Cell. Biol. *9*, 4545–4549.

37. Adjei, A.A. (2001). Blocking oncogenic Ras signaling for cancer therapy. J. Natl. Cancer Inst. *93*, 1062–1074.

38. Waeber, G., Delplanque, J., Bonny, C., Mooser, V., Steinmann, M., Widmann, C., Maillard, A., Miklossy, J., Dina, C., and Hani, E.H. (2001). The gene MAPK8IP1, encoding islet-brain-1, is a candidate for type 2 diabetes. Nat. Genet. *24*, 291–295.

39. Johnson, P.R., Burgess, J.K., Underwood, P.A., Au, W., Pomiris, M.H., Tamm, M., Ge, Q., Roth, M., and Black, J.L. (2004). Extracellular matrix proteins modulate asthmatic airway smooth muscle cell proliferation via an autocrine mechanism. J. Allergy Clin. Immunol. *113*, 690–696.

40. Mohiddin, S.A., Ahmed, Z.M., Griffith, A.J., Tripodi, D., Friedman, T.B., Fananapazir, L., and Morell, R.J. (2004). Novel association of hypertrophic cardiomyopathy, sensorineural deafness and a mutation in unconventional myosin VI (MYO6). J. Med. Genet. *41*, 309–314.

41. Arellano-Llamas, A., Garcia, F.J., Perez, D., Cantu, D., Espinosa, M., De la Garza, G., Maldonado, V., and Melendez-Zajgla, J. (2006). High Smac/DIABLO expression is associated with early local recurrence of cervical cancer. BMC Cancer *6*, 256.

42. Eshed, Y., Feinberg, K., Poliak, S., Sabanay, H., Sarig-Nadir, O., Bermingham, J.R., and Peles, E. (2005). Gliomedin mediates Schwann cell-axon interaction and the molecular assembly of the nodes of Ranvier. Neuron *47*, 215–229.

43. Farmer, S.R. (2006). Transcriptional control of adipocyte formation. Cell Metab. *4*, 263–273.

44. Das, C., Hizume, K., Batta, K., Kumar, B.R., Gadad, S.S., Ganguly, S., Lorain, S., Verreault, A., Sadhale, P.P., Takeyasu, K., et al. (2006). Transcriptional coactivator PC4, a chromatin-associated protein induces chromatin condensation. Mol. Cell Biol. *26*, 8303–8315.

Accession Numbers